International Journal of Science and Research (IJSR)
ISSN: 2319-7064
ResearchGate Impact Factor (2018): 0.28 | SJIF (2019): 7.583

Simulation of a Full PWR Core with MCNP6

Mohga Hassan

Safety Engineering Department, Nuclear and Radiological Regulatory Authority, Cairo, Egypt
Mohgaig[at]yahoo.com

Abstract: ***The advantages for using Monte Carlo method to analyze full-core reactor configuration include exact representation of geometry and physical phenomena that are important for reactor analysis. The accuracy of the simulation will depend on the degree of details considered in the model. In this work, the Monte Carlo code MCNP6 is used to simulate two full PWR cores with detailed geometry at hot zero power. The simulated models are verified against actual reactor measurements provided in a published benchmark. Measurements include control banks worth and effective multiplication factor at different control banks insertions and boron concentrations. The isothermal temperature coefficient is also evaluated. Integrated thermal flux at detector positions is evaluated and compared to the actual data provided by the benchmark. Axial thermal flux calculated for selected assemblies was compared to the results produced by detector signals. The accuracy of thermal flux calculations were evaluated using two methods; the absolute relative difference and the root mean square deviation.***

Keywords: MCNP6, PWR, Thermal flux, Control rod worth, ITC, Radial flux, Axial flux

1. Introduction

The advantages of the Monte Carlo method for reactor analysis are well known. Continuous energy Monte Carlo codes such as MCNP6 [1] are capable in principle of analyzing reactor configurations with arbitrary geometrical complexity , limited by the ability of the code (and patience of the user) to represent arbitrary shapes in a computational model; and limited by the knowledge of cross sections that describe the physical phenomena being modeled. In addition to the flexibility of Monte Carlo to simulate the most complex geometry, continuous energy Monte Carlo treats neutron energy dependence correctly with essentially no approximations [2]. Moreover, previous work has demonstrated that Monte Carlo methods can be made to run efficiently on most if not all production computer architectures that have been introduced to date [3].

Benchmark problems are a major method to verify code models; examples are references [4-7]. These benchmarks, while using full-core simulations and measured data, take the approach of reducing the benchmark to single-assembly calculations and do not provide detailed full-core tests or measured reactor data [8]. The BEAVRS benchmark (Benchmark for Evaluation and Validation of Reactor Simulations) provides the most detailed specifications, to allow a challenging comparison of a whole core model for neutronics calculations. It was published in 2013 by the Massachusetts Institute of Technology (MIT) Computational Reactor Physics Group (CRPG), and it was updated several times [8-10].This benchmark provides a detailed description of a four loop Westinghouse PWR loaded with 193 fuel assemblies of 17×17 lattice for the rated reactor power of 3411 MWth. The benchmark also provides measured reactor data for Hot Zero Power (HZP) physics tests, including multiplication factor at different control banks insertions and boron concentration, control banks worth, and isothermal temperature coefficient (ITC). Detector readings, in the form of three-dimensional in-core flux maps from fifty-eight instrumented assemblies, are provided. These in-core detector signals are axial thermal neutron flux distributions measured by fission chambers inserted into the instrumentation tube of the 58 assemblies in the core. Both the axially-integrated and axial distributions of the thermal neutron flux are reported.

Many research studies have been performed using the BEAVRS benchmark [11-18]; none of which used MCNP code in the simulation. In the present work two BEAVRS benchmarks [8,10] are simulated using MCNP6 Monte Carlo Code [1] at HZP; the differences between the two cores are clarified in the next section. The model is used to calculate multiplication factor (estimated at different control banks insertions and boron concentrations), control bank worth, and ITC. Axially integrated thermal flux for 58 assemblies resembling detector positions in the core, are also evaluated and compared to the actual results provided by the benchmark. Moreover, axial relative flux for selected assemblies is estimated and compared to actual data located at 61 axial positions of assemblies with detectors.

2. Core Description and Modifications

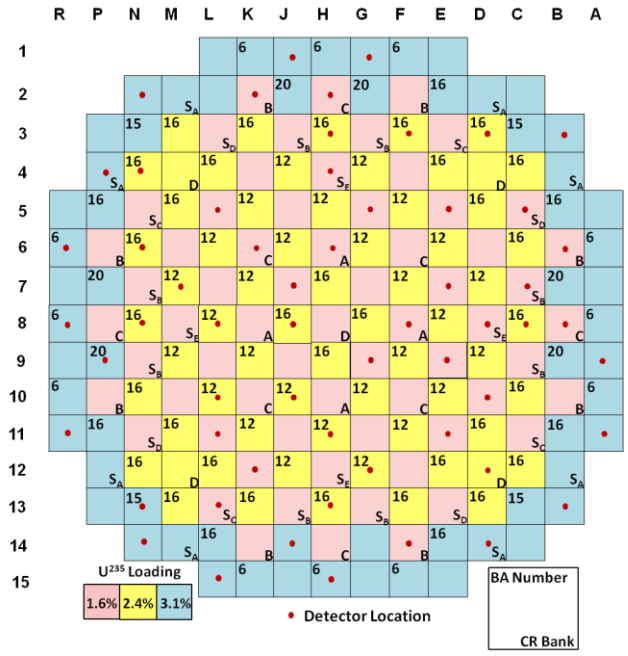

Figure 1: Core Arrangement for BEAVRS Benchmark

A presentation of core arrangement, used in BEAVRS benchmarks, including ^{235}U enrichment, number and location of burnable absorber (BA) and control rod (CR) banks distribution in the core, as well as location of detectors are illustrated in figure 1, and the main specifications for the core are listed in table 1. Details of data concerning design and material composition can be found in the reference documents [8-10].

Table 1: BEAVRS Main Core Specification

Core	
Thermal power	3411 MW
Operating pressure	2250 psia
Fuel assembly	
Number	193
Lattice	17×17
Assembly pitch	21.50364 cm
Active fuel length	365.76 cm
Fuel rod pitch	1.25984 cm
No. of fuel rods	264
Fuel Rod	
Pellet material	UO2
Cladding material	Zircaloy
U-235 enrichment	1.6, 2.4, 3.1 wt %
Pellet radius	0.39218 cm
Cladding material	Zircaloy
Inner clad radius	0.40005 cm
Outer clad radius	0.45720
Control rod	
BV1[8]	B_4C
BV2[10]	
Upper region (259 cm)	B_4C
Lower region (102 cm)	Ag-In-Cd
Burnable absorber	Borosilicate glass
Spacer grid	
Number	8
Material for fuel rod	Inconel 718, Zircaloy
Material for assembly	SS.304, Zircaloy
Structure Material	
Baffle	SS.304
Core Barrel	SS.304
Neutron shield	SS.304
Pressure vessel	Carbon Steel 508

There are major differences between the first and last version of this benchmark (BV1 and BV2). The modifications are listed in the following:

- In BV2, the coolant in the nozzle and support plate structures has different temperatures and densities from that in the core. In the BV1 core, the coolant temperature and density were set to 566.5 ^{o}K and 740.6 kg/m^3, respectively. While in the BV2, the coolant temperature and density in the nozzle and support plate were updated to 349.1 ^{o}K and 981.0 kg/m^3 ^{o}K, respectively, and the rest is like BV1.
- In the BV2 model, the fuel is lifted by 0.741 cm with no change in active fuel length.
- The main active burnable absorber length did not change, but it was shifted down 0.529 cm in BV2.
- The part under the bottom of the burnable absorber rod in BV1 was water in the lower part of the guide tube, while in BV2, the bottom part of the absorber rod is stainless steel (SS) pin introduced as an end plug. In addition, the air which filled the two gaps in the burnable absorber rods of BV1 had been replaced by helium in BV2.
- The plenum region of the burnable absorber was also changed from SS pin in BV1 (33.677 cm) to be replaced in BV2 by two parts; a hollow part that contains air (20.294 cm), directly above burnable absorber rod, then SS pin (10.344cm).
- Positions of spacer grids are slightly different, details can be found in references 8, 10.
- Considering the control rods, the control rod material was only Silver Indium Cadmium (Ag-In-Cd) in BV1. In BV2, the control rods are divided into two parts, an upper part of about 259 cm has boron carbide (B_4C) as an absorber, while the lower part of about 102 cm has Ag-In-Cd absorber.

3. Model Description

A detailed full core of the benchmark design was simulated using MCNP6 Code [1], and the Evaluated Neutron Data File library, ENDF/B-VII.1 [19].The MCNP6 model, for BV2, is illustrated in figure 2. The model was prepared to include all the details like spacer grids, neutron shield, upper and lower nozzles, and upper plenum. There are nine types of fuel assemblies in the initial core, according to fuel enrichment, presence of burnable absorbers and control rods (see figure 1).

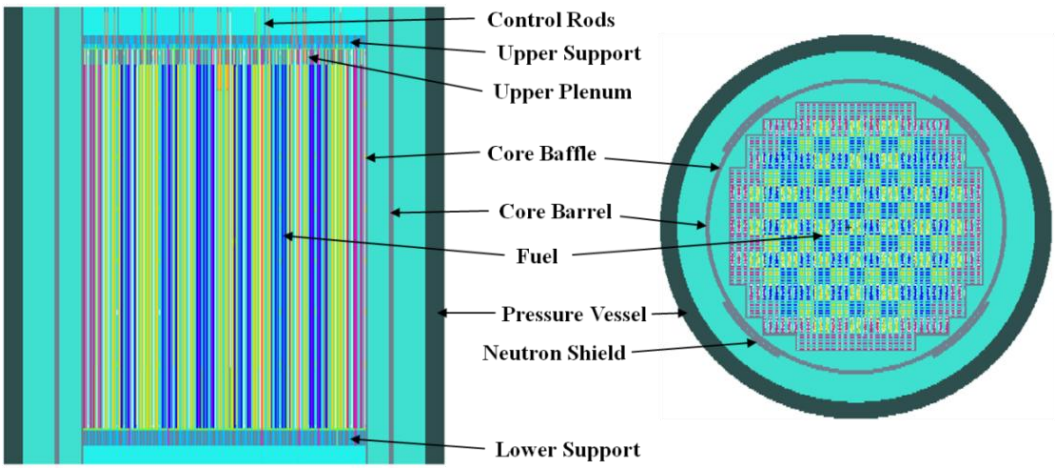

Figure 2: MCNP Model of BEAVRS Benchmark

175 million neutron histories (500,000 neutron per cycle, 150 skipped cycles, and 350 active cycles) were used to perform the calculations. The standard deviation of the criticality calculation was 0.00006. The benchmark provided conditions for HZP flux calculation; they are stated in table 2. The control rod step is equal to 1.5817 cm.

Table 2: Hot Zero Power Conditions

Core Power	25 MWth
Inlet Coolant Temperature	560^0F
Rod Bank A Position	Step 228
Rod Bank B Position	Step 228
Rod Bank C Position	Step 228
Rod Bank D Position	Step 213
Boron Concentration	975 ppm

The reactivity change, due to change of temperature, density, or control bank insertion, is calculated from [20]:

$$\delta\rho = \frac{K_2 - K_1}{K_2 \times K_1} \quad (1)$$

Where $\delta\rho$ is the change in reactivity, K_1 is the multiplication factor before change and K_2 is the multiplication factor after change.

The ITC is the sum of moderator temperature coefficient (MTC) and fuel temperature coefficient (FTC)[21]. The MTC or FTC, are calculated by using the following equation [20]:

$$MTCorFTC = \frac{\delta\rho}{T_2 - T_1} \quad (2)$$

Where $\delta\rho$ is estimated using equation 1with K_1 is the multiplication factor at original temperature and K_2 is the multiplication factor after temperature raise. T_2 is the elevated temperature and T_1 is the original temperature.

The accuracy of the calculation of thermal flux and power distribution was evaluated by two factors; the first is the absolute relative difference (ARD) given by [22]:

$$ARD = \frac{|calculatedvalue - referencevalue|}{referencevalue} \quad (3)$$

And the other is the root mean square (RMS) given by [23]:

$$RMS = \sqrt{\frac{\sum_{i=1}^{N}(calculatedvalue - referencevalue)^2}{N}} \quad (4)$$

Where N is the number of calculated values

4. Results and Discussion

4.1 Effective multiplication factor

Effective multiplication factor was calculated for different control banks insertions and corresponding boron concentration provided in the benchmark for each case [8, 10]. The results are shown in table 3, the difference between benchmark results and present results is shown between brackets, considering that measured k_{eff} equals 1. It is clear that the MCNP6 model is capable of predicting the multiplication factor for each case with acceptable accuracy. The results also show that BV2 is capable of producing better results that are closer to the benchmark values.

Table 3: Results of Criticality for Provided Conditions

Configuration	Boron Concentration (pcm)	BV1	BV2
ARO (All Rods Out)	975	0.99816 (-184)	0.9996 (-40)
D in	902	0.99774 (-226)	1.00123(123)
C,D in	810	0.99787 (-213)	1.00037 (37)
A, B, C, D in	686	0.99714 (-286)	0.99927 (-73)
A,B,C,D,SE, SD,SC in	508	0.99655 (-345)	0.99798 (-202)

4.2 Control bank worth

The control Bank worth was calculated by considering the difference in criticality with all rods out and that with all control rods bank (or banks) in. Table 4 shows that the resulting control banks worth agree to a large extent with actual values, the largest difference is for banks (C, D) insertion, 65 pcm for BV1(5.4%) and 47 pcm for BV2 (3.9%) , and it can be seen that BV2 has better results than BV1.

Table 4: Comparison of Control Rod Bank Worth Between MCNP6 Results and Benchmark Data

Configuration	BV1 (pcm)	BV2 (pcm)	Measured (pcm)
D in	756	775	778
C,D in	1138	1250	1203
A, B, C, D in	501	558	548
A,B,C,D,SE, SD,SC in	1082	1110	1099

4.3 Isothermal temperature coefficient

In order to estimate the ITC, multiple runs were performed where the moderator temperature and the fuel temperature were raised by 5 ^{o}K, Calculations were all performed at a boron concentration of 975ppm. The results are shown in table 5.

Table 5: Comparison of ITC Between Calculation Results and Measurement (pcm/^{o}K)

Case	MTC	FTC	ITC
BV1	-2.03	-2.17	-4.20
BV2	-1.85	-1.92	-3.77
Measured	-	-	-3.15

4.4 Thermal flux

Thermal flux was estimated in 58 assemblies where the detectors are positioned (see Fig.1). F4 tally of MCNP6 was used to estimate thermal flux and then, the flux was then normalized to the average flux in 58 assemblies ($\sim 1.4\times10^{14}$n/cm^2.sec). The results of the calculations are shown in figures 3 and 4. The maximum ARD occurred at assembly B13 for BV2 (0.156). Despite the lower value of maximum ARD; BV1 have higher RMS, 6.9%; whereas it is equal to 5.3% for BV2. The results are in agreement with measured results as well as most of other codes results, where in some cases difference between calculated and measured results reached 0.165 and RMS 6.89% [17].

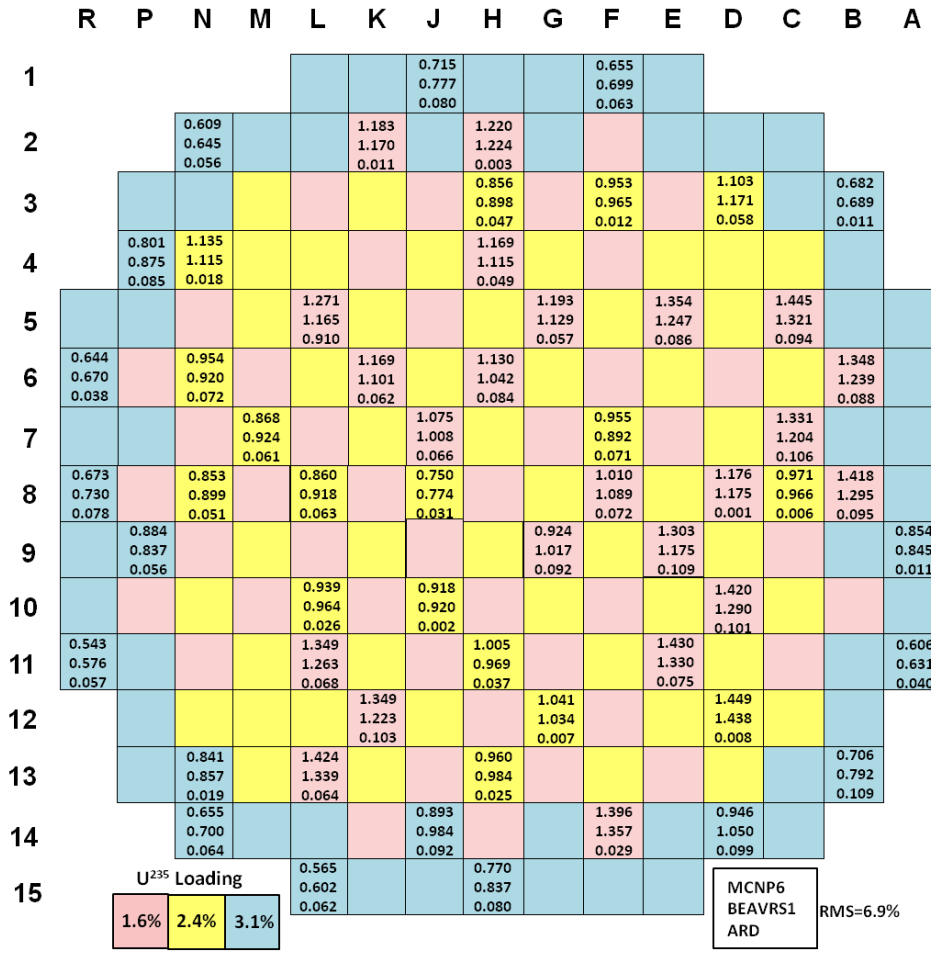

Figure 3: Normalized Thermal Flux for BV1

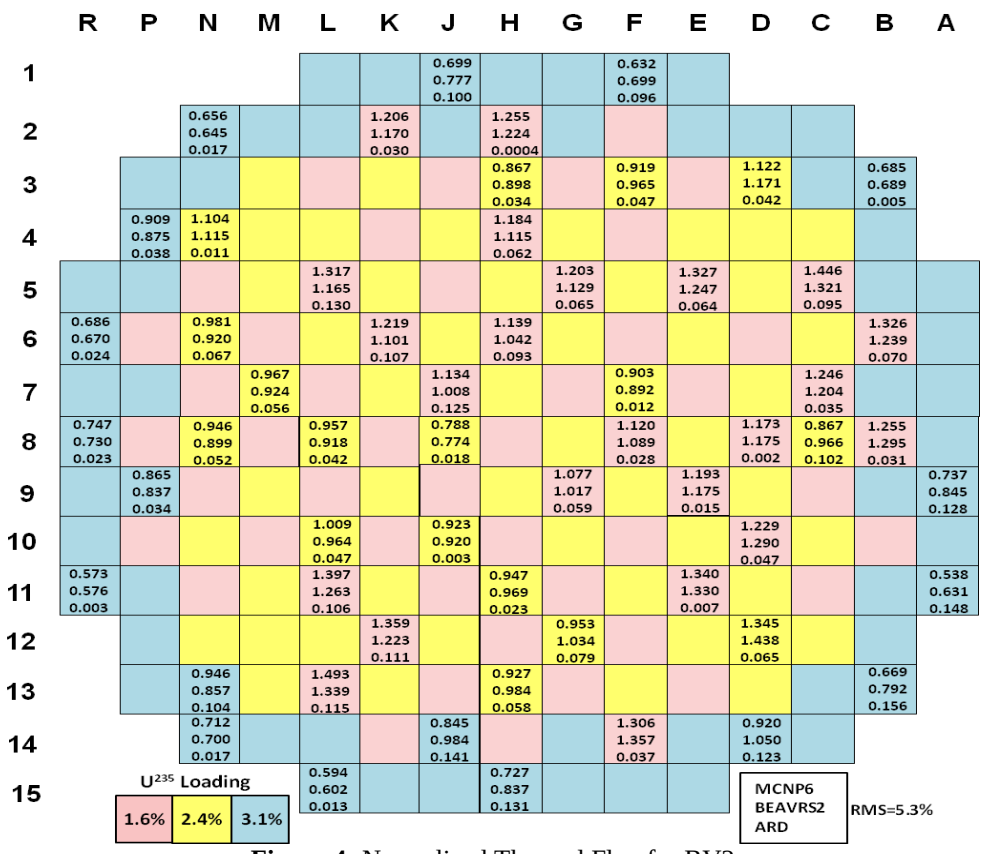

Figure 4: Normalized Thermal Flux for BV2

Another means to verify the simulation is by comparing the axial relative thermal flux to the measured values. Figure 5 illustrates the relative axial flux for six assemblies distributed in the core; N2, H2, G9, L10, E11, and B13. These assemblies were chosen to have different positions, different relative flux and different ARD values, and included assembly B13 with the maximum ARD. The assemblies were divided into 61 axial divisions, corresponding to the number of detector positions in the benchmark. The flux was calculated for each division, and then it is normalized by dividing each segment flux by the average of all 58 assemblies. The results were compared to normalized detector readings provided in the benchmark. It can be seen that there is a reasonable agreement between the calculated and measured distributions, and that BV2 has results that are closer to real values than BV1.

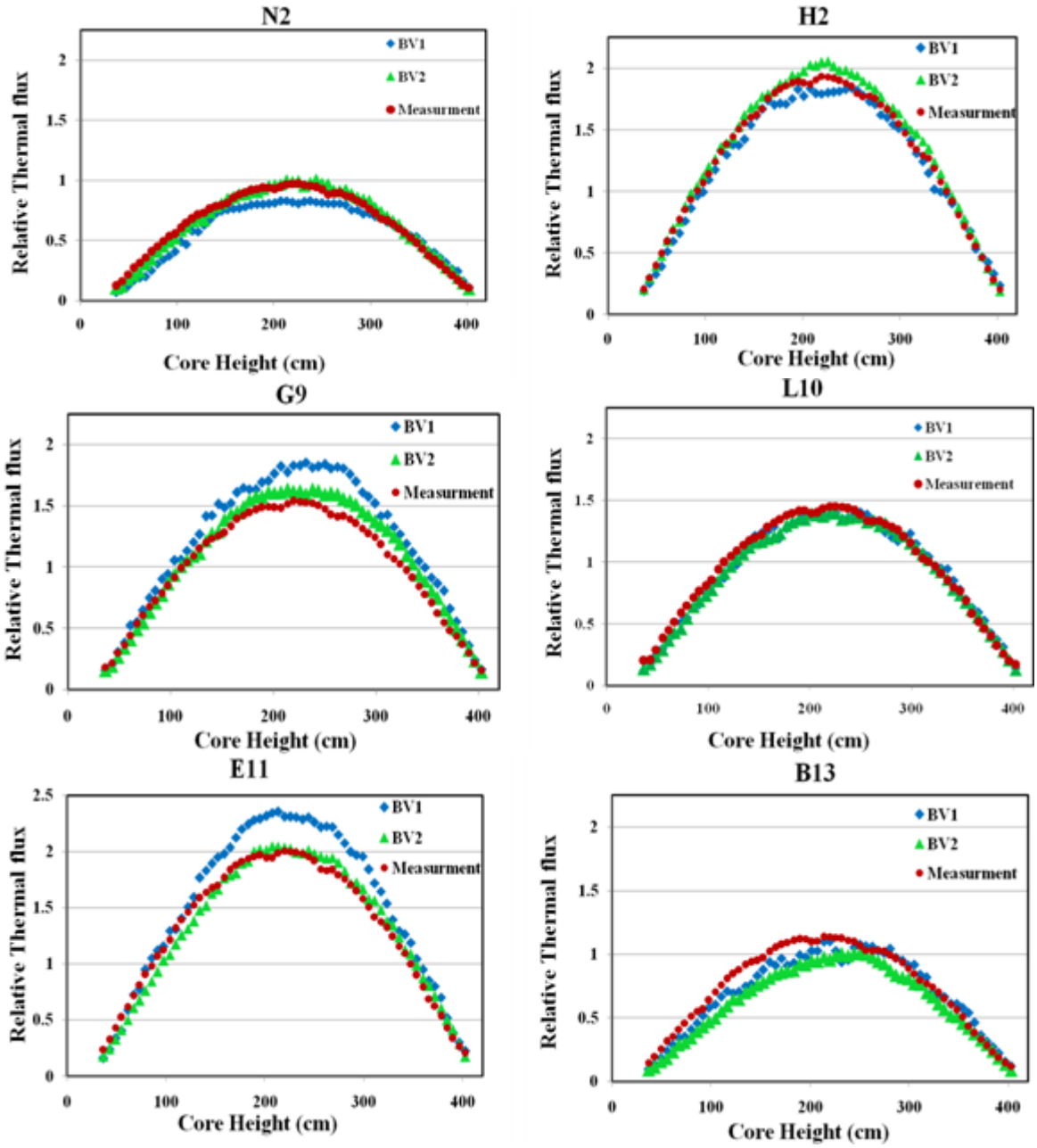

Figure 5: Normalized Axial Flux for Selected Assemblies in Comparison to Fission Chamber Measurements

5. Conclusions

- In the present work, two models of PWR were simulated based on BEAVRS benchmark using MCNP6 Monte Carlo code. The simulation included comprehensive description of fuel assemblies, as well as design details like baffle and barrel, upper and lower nozzles, upper plenum and also spacer grids.
- The results included the multiplication factor, at various control banks insertions, and boron concentrations. The resulted differences from benchmark values were within acceptable range.
- The maximum difference between the calculated values and benchmark values for control rod worth was less than 5.4% for BV1 and 3.9% for BV2.

- The isothermal temperature coefficient was calculated by adding the MTC and FTC. The comparison between calculation and actual results was satisfactory.
- Fifty eight assemblies containing detectors were divided into 61 axial divisions where thermal flux was estimated, integrated, and compared to the actual data. The maximum ARD occurred at assembly B13 for BV2 with a value of 0.156. The RMS for BV1 was 6.9% and for BV2 was 5.3%
- Axial relative thermal flux was compared to real data resulting from 61 axial detector positions, for six assemblies distributed in the core including the one with highest ARD.
- The simulation of modified version of the BEAVRS benchmark (BV2) yielded more realistic results than the simulation of the first version (BV1).

References

[1] Pelowitz, D.B, "MCNP6 User's Manual Version 1.0, Los Alamos National Laboratory report, LA-CP-13-00634, Rev. 0, (2013).
[2] WILLIAM R. MARTIN, " Challenges and Prospects for Whole-Core Monte Carlo Analysis", NUCLEAR ENGINEERING AND TECHNOLOGY, VOL.44 NO.2 MARCH 2012
[3] F. B. Brown, "Recent Advances and Future Prospects for Monte Carlo," Proc. Joint International Conference on Supercomputing in Nuclear Applications and Monte Carlo 2010 (SNA + MC2010), Tokyo, Japan, October 17-21, 2010.
[4] OECD/NEA. International Reactor Physics Benchmark Experiments (IRPhE), May 2012. ISBN 978-92-64-99168-2.
[5] K.S. Smith, S. Tarves, T. Bahadir, and R. Ferrer. Benchmarks for Quantifying Fuel Reactivity Depletion Uncertainty. Technical Report 1022909, Electric Power Research Institute, 2011.
[6] Benchmark on Deterministic Transport Calculations Without Spatial Homogenisation. Technical Report NEA/NSC/DOC(2005)16, NEA No. 5420, 2005. ISBN 92-64-01069-6.
[7] S. Douglass, F. Rahnema, and J. Margulies. A stylized three dimensional PWR whole-core benchmark problem with Gadolinium. *Annals of Nuclear Energy*, 37(10):1384 – 1403, 2010.
[8] MIT Computational Reactor Physics Group. (2013). BEAVRS – benchmark for evaluation and validationof reactor simulations. Rev. 1.1.1. Cambridge, UK:MIT CRPG.
[9] MIT Computational Reactor Physics Group. (2017).BEAVRS – benchmark for evaluation and validationof reactor simulations. Rev. 2.0.1. Cambridge, UK:MIT CRPG
[10] MIT Computational Reactor Physics Group. (2018). BEAVRS – benchmark for evaluation and validation of reactor simulations. Rev. 2.0.2. Cambridge, UK: MIT CRPG
[11] JaakkoLeppänen , RikuMattila , and Maria Pusa, "Validation of the Serpent-ARES code sequence using the MIT BEAVRS benchmark – Initial core at HZP conditions", (2014) Annals of Nuclear Energy Vol.69, 212–225.
[12] Kelly,D.J., Aviles,B.N., Romano,P.K., Herman,B.R.,Horelik,N.E., Forget,B., (2014), "Analysis of Select BEAVRS PWR Benchmark Cycle 1 Results Using MC21 and OpenMC", PHYSOR 2014 – The Role of Reactor Physics towards a Sustainable Future September 28 – October 3, 2014.
[13] Cho, H.H and Joo, H.G.,(2015) "Solution of the BEAVRS benchmark using the nTRACER direct whole core calculation code", Journal of Nuclear Science and Technology, Vol. 52, Nos. 7–8, 961–969.
[14] Liang, J., Wang, K., Yu, G., et al.,(2013)"JMCT Monte Carlo analysis of BEAVRS benchmark: hot zero power results",. ActaPhysicaSinica–Chinese Edition- 65(5).
[15] Wang, Z., Wu, B.,Hao, L., Liu, H., Song, J., (2018),"Validation of SuperMC with BEAVRS benchmark at hot zero power Condition", Annals of Nuclear Energy 111; 709–714
[16] Bykov,V.,Vasiliev, A., Ferroukhi, H.,Pautz,A., (2016), " Solution of the BEAVRS Benchmark Using CASMO-5 / SIMULATE-5 Code Sequence", PHYSOR 2016 – Unifying Theory and Experiments in the 21st Century, May 1–5, Sun Valley, ID, USA. Pages 1960-1968.
[17] Darnowski, P., andPawluczyk, M.,(2019), "Analysis of the BEAVRS PWR benchmarkusing SCALE and PARCS", NUKLEONIKA ;64(3):87-96.
[18] Chadwick,M.B., et.al, ENDF/B-VII.1 Nuclear Data for Science and Technology: Cross Sections, Covariance, Fission Product Yields and Decay Data, (2011).
[19] Cacuci, D.G.,"Handbook of Nuclear Engineering", Springer Science & Business Media LLC 2010,pp. 1723-2822
[20] Tsuji, M., Aoki, Y., Shimazu, Y., Yamasaki, M., And Hanayama, Y.,(2006), "Estimating Temperature Reactivity Coefficients by Experimental Procedures Combined with Isothermal Temperature Coefficient Measurements and Dynamic Identification", Journal of NUCLEAR SCIENCE and TECHNOLOGY, Vol. 43, No. 5, p. 576–586.
[21] Bennett, J., and Briggs, W., (2015), "Using & Understanding Mathematics A Quantitative Reasoning Approach", Pearson Education, p.124.
[22] SPIEGEL, M.R., and STEPHENS, L.J., (2008) "Theory and Problems of Statistics", McGraw-Hill Companies, p66.